Spring 2008

Fabrication of long-period fiber gratings by CO_2 laser irradiation for high temperature applications

Tao Wei

Department:

FABRICATION OF LONG-PERIOD FIBER GRATINGS BY CO_2 LASER IRRADIATION FOR HIGH TEMPERATURE APPLICATIONS

by

TAO WEI

A THESIS

Presented to the Faculty of the Graduate School of the

MISSOURI UNIVERSITY OF SCIENCE AND TECHNOLOGY

In Partial Fulfillment of the Requirements for the Degree

MASTER OF SCIENCE IN ELECTRICAL ENGINEERING

2008

Approved by

Dr. Hai Xiao, Advisor
Dr. Steve Watkins
Dr. Hai-Lung Tsai

ABSTRACT

Long period fiber gratings (LPFG) have unique advantages such as small insertion loss, low retro-reflection, good sensory property and low cost fabrication. LPFGs have found many applications in optical fiber communications as well as in optical fiber sensors. Recently, high-performance LPFGs have been successfully fabricated by CO_2 laser irradiations. The unique thermal stability enables many potential sensing applications in high temperature environments.

In this thesis, the CO_2 laser based LPFG fabrication system with in-situ monitoring has been demonstrated. High quality LPFGs were successfully fabricated using the system. The transmission spectra of the LPFGs possessed a strong attenuation (>25dB), a negligible device loss (<1dB) and a narrow FWHM (~7 nm). The resonance wavelength showed a linear dependence on grating periods as predicted by the Bragg condition. An interferometric method was developed to measure the refractive index change caused by CO_2 laser irradiation, which helped tune the laser parameters to optimize the fabrication process. High temperature performance and survivability of the fabricated LPFGs were evaluated systematically. It has been found that the thermal shock process could dramatically improve the thermal stability of the LPFG device.

Two chemical sensing applications of LPFG were demonstrated. In the first one, the ambient refractive index sensing ability of bare LPFG was examined. The experimental data showed a good agreement with the simulation results. In the second one, the Palladium coated LPFG was used to monitor the concentration of hydrogen gas at different temperatures ranging from 25°C to 200°C. The sensitivity, response time and repeatability have been tested.

ACKNOWLEDGMENTS

I would like to take this opportunity to thank all those people who helped me with the successful completion of my research. First, I would like to express my gratitude to my advisor Dr. Hai Xiao, without who this research could be considered incomplete. I thank him for giving me a chance to work with him and for his continued support with valuable advice and encouragement. His subtle guidance with unbelievable patience has made a great impact on this research and me.

I am grateful to Dr. Steve Watkins, Department of Electrical and Computer Engineering and Dr. Hai-Lung Tsai, Department of Mechanical and Aerospace Engineering for being my committee members.

Additional gratitude is owed to John Montoya who I worked with on this project and who gave me lots of precious advice.

I also would like to take this opportunity to thank my colleagues in my group for being supportive all the time.

I would also like to thank my parents for everything they have done for me. Finally, I would like to thank the sponsors for this project. They are the U.S. Department of Energy through the National Energy Technology and the Office of Naval Research through the Young Investigator Program.

TABLE OF CONTENTS

Page

ABSTRACT iii

ACKNOWLEDGMENTS iv

LIST OF ILLUSTRATIONS vii

SECTION

1. INTRODUCTION 1
   1.1. BACKGROUND 1
      1.1.1. General Characteristics 2
      1.1.2. Fabrication Techniques 4
      1.1.3. Applications 4
   1.2. RESEARCH OBJECTIVE 5
   1.3. THESIS OVERVIEW 5
2. FABRICATION AND BASIC TRANSMISSION CHARACTERISTICS 7
   2.1. FABRICATION 7
   2.2. TRANSMISSION CHARACTERISTICS 9
      2.2.1. Typical Transmission Spectra 9
      2.2.2. Typical Transmission Spectra with Different Periods 10
   2.3. SUMMARY 11
3. HIGH TEMPERATURE PERFORMANCE AND IMPROVEMENT 12
   3.1. HIGH TEMPERATURE SURVIVABILITY 12
   3.2. THERMO STABILITY AND IMPROVEMENT 13
      3.2.1. Annealing 13
      3.2.2. Thermal Shock 14
   3.3. SUMMARY 14
4. REFRACTIVE INDEX MODULATION MEASUREMENT 15
   4.1. MEASUREMENT THEORY 15
      4.1.1. CO_2 Laser Exposure Profile Approximation 15
      4.1.2. Measurement Principle 16
   4.2. EXPERIMENT 18

4.3. RESULTS AND DISCUSSIONS 18
4.4. SUMMARY 20
5. APPLICATIONS 21
5.1. AMBIENT REFRACTIVE INDEX MEASUREMENT 21
5.2. PALLADIUM COATED LPFG FOR HYDROGEN SENSING 22
5.2.1. Introduction. 22
5.2.2. Principle of Operation. 22
5.2.3. Experiment Setup. 23
5.2.4. Result and Discussion. 24
5.3. SUMMARY 28
6. CONCLUSION 30
BIBLIOGRAPHY 33
VITA 37

LIST OF ILLUSTRATIONS

Figure Page

1.1 Coupling between the guided core mode and the cladding modes in a LPFG 2

1.2 Transmission response of a typical LPFG 3

2.1 Schematic setup of the CO_2 laser based LPFG fabrication system 8

2.2 Photograph of LPFG fabrication system..... 8

2.3 Measured and simulated transmission spectra of a LPFG with a period of 535μm 9

2.4 LPFG transmission spectra with different periods..... 10

2.5 Resonance wavelength as a function of period..... 11

3.1 Test of LPFG at various temperatures 12

3.2 Thermo stability tests and improvement..... 13

4.1 Setup schematic of measurement..... 15

4.2 Fiber optic Michelson interferometer to measure refractive index modulation 16

4.3 Results of refractive index modulation measurement..... 19

5.1 LPFG in response to ambient refractive index changes..... 21

5.2 Schematic of Pd-LPFG in-situ measurement for hydrogen concentration sensing 23

5.3 SEM image of Pd-coated LPFG 25

5.4 Spectrum of LPFG coated with Pd in 8% H_2 and H_2 free atmosphere 26

5.5 Wavelength shift as a function of H_2 concentration at various temperatures 27

5.6 Response time and recovery time of LPFG in 4% H_2 28

5.7 Repeatability test of Pd-LPFG 29

1. INTRODUCTION

1.1. BACKGROUND

Optical fiber-based devices are wildly used in optical communications and sensing applications. Within optical communication networks, optical fiber-based devices perform such critical operations as coupling/splitting, wavelength-selective filtering, and optical switching [1-4]. In the field of optical sensing, optical fiber sensors, with unique advantages such as immunity to electromagnetic interference, high sensitivity, resistance to corrosion, and high temperature survivability, are widely used to measure various physical (e.g., stress, temperature, pressure, refractive index, etc.) and chemical (e.g., pH, chemical concentration, humidity, etc.) parameters [5].

Fiber gratings are among the most popular devices that have been widely used in both optical communications and optical fiber sensing. There are two types of fiber gratings have been developed so far including the fiber Bragg grating (FBG) and the long period fiber grating (LPFG).

A FBG consists of a periodic variation in the refractive index of an optical fiber, with the period being on the order of hundreds of nanometers. FBGs couple light from a forward-propagating core-guided mode to a backwards-propagating core-guided mode near a resonant wavelength, in effect acting as wavelength-selective mirrors [6]. In an LPFG, the periodic refractive index perturbation in the fiber core has a period in the hundreds of micrometers, coupling the guided light inside fiber core into the cladding modes (known as the lossy modes), at certain discrete wavelengths (commonly referred as to the resonance wavelengths). A LPFG has been used for many applications including flattening the gain spectrum of erbium-doped fiber amplifiers, monitoring power levels transmitted in optical fibers, and compensating dispersion in an optical communication system [7-9].

LPFGs have been traditionally fabricated by exposing photosensitive optical fiber to ultraviolet (UV) light transversely either through an amplitude mask or point-by-point to create a periodic refractive index change inside an optical fiber. Unfortunately, the UV-induced refractive index change inside an optical fiber can only survive at a

relatively low temperature. As a result, the UV exposure fabricated LPFGs are not suitable for high temperature applications.

More recently, LPFGs have been fabricated by a variety of other techniques including exposure to carbon-dioxide (CO_2) laser light [1] and electronic arcs. The physical process by which the refractive-index change is induced in an optical fiber during exposure to CO_2 laser light gives these LPFGs unique properties compared to the traditional LPFGs fabricated by exposure to UV light. It has been reported that the CO_2 laser induced LPFGs can survive a temperature higher than 1200°C [10-12]. The high temperature capability makes the CO_2 laser fabricated LPFG a good platform for many sensing applications involving high temperature harsh environments.

1.1.1. General Characteristics. An LPFG consists of a periodic spatial variation (along the fiber longitudinal axis) in the refractive index of an optical fiber. The periodic refractive index modulation couples light from a forward-propagating core-guided mode to forward-propagating cladding-guide modes near certain resonance wavelengths [7]. The light coupled into the cladding modes eventually attenuates due to the high loss of the cladding modes. As a result, the transmission spectrum of a LPFG has a series discrete attenuation bands near the resonance wavelengths.

Grating periods for LPFGs are commonly in the hundreds of micrometers to produce resonance wavelength in the communication wavelength centered around 1550nm. As shown in Fig. 1.1, for LPFGs inscribed in single-mode fiber (SMF), mode coupling happens when phase-matching condition between the fundamental core mode

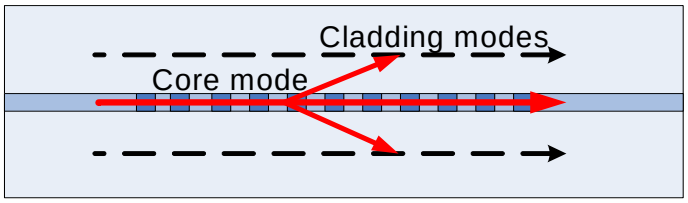

Figure 1.1 Coupling between the guided core mode and the cladding modes in a LPFG

and a particular cladding mode is satisfied. The phase-matching condition required for coupling is given by

$$\beta_{core} - \beta_{clad}^{mn} = \frac{2\pi}{\Lambda} \tag{1.1}$$

where β_{core} is the propagation constant of core mode, known as the fundamental linearly polarized (LP01) mode, the β_{clad}^{mn} is the propagation constant of cladding modes (LPmn) and Λ is the period of LPFG.

An alternative form of the phase-matching condition is given by

$$\lambda_{re}(n_{core} - n_{clad}^{mn}) = \Lambda \tag{1.2}$$

where n_{core} is the effective index of the guided core-mode, n_{clad}^{mn} is the effective index of the LP_{mn} cladding mode, and λ_{re} is the center wavelength of the transmission resonance. The light traveling in cladding modes experiences a high loss, which gives attenuation bands at resonance wavelengths in the transmission spectrum. The typical transmission spectrum of a typical LPFG is shown in Fig. 1.2.

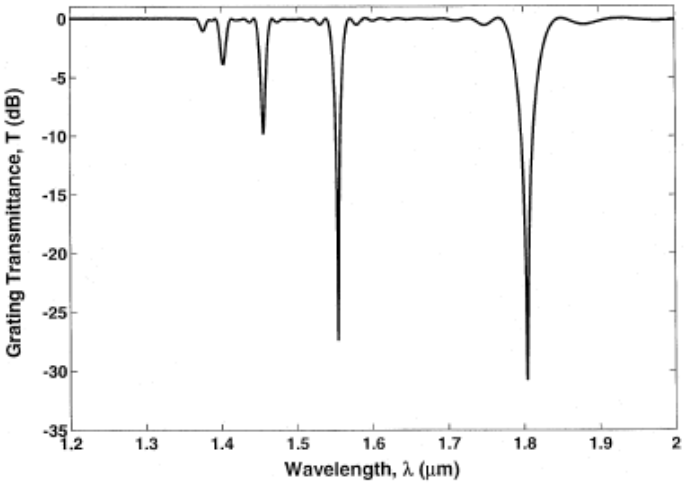

Figure 1.2 Transmission response of a typical LPFG

1.1.2. Fabrication Techniques. A number of techniques have been developed for fabricating LPFGs in addition to exposing photosensitive optical fibers to UV light. Electric arc discharge and focused infrared femtosecond laser pulses have both been used to write LFPGs on a point-by-point basis. Both of the two methods can achieve a permanent density variation on optical fiber which helps create a permanent modification of the refractive index of the core periodically [13-16]. LPFGs have also been created by ion implantation (bombardment) through a metal amplitude mask. Though a graded mask, ion implantation of silica glass increases the refractive index of optical fiber in a periodic pattern achieving LPFGs [17]. Hollow-core optical fiber filled with a liquid crystal solution can be periodically poled (spatially) by applying voltage to electrodes to create an LPFG structure [18]. Pressing on an optical fiber with a grooved plate is another method by which an LPFG can be temporarily created. This is based on the physical deformation on optical fiber which also changes the refractive index of the fiber core [19, 20]. Most recently, the CO_2 laser irradiation methods have been developed, which is the method discussed in this paper [10, 11].

1.1.3. Applications. Initial investigations involving LPFGs indicated that they could be useful in a variety of applications. Both active and passive LPFG-based devices have been reported in the literature, of which, besides communication applications, a small representative number for the interest of optical sensing applications are mentioned here. The high sensitivity of cladding modes to surrounding refractive index values makes LPFGs suitable for chemical sensing such as gas concentration or environmental measurements [21-28]. Meanwhile, since bending, stress, torsion and temperature can affect on LPFGs, physically change the system and cause a resonant wavelength shift correspondingly, it has been widely reported that LPFGs can be used for bending, stress, torsion and temperature sensing [29-33]. All these sensing applications are unique because the all-glass structure helps these devices survive extreme conditions such as corrosion and high temperature (1200ºC) [10-12].

1.2. RESEARCH OBJECTIVE

The main objective of this thesis is to study using a CO_2 laser to fabricate LPFGs and develop chemical sensors using the fabricated LPFGs, especially for applications involving high temperature harsh environments. To be detailed, the specific objectives are:

1. Build a CO_2 laser-based system with the in-situ monitoring capability to fabricate high performance LPFGs,

2. Evaluate and improve the thermal stability of LPFGs,

3. Characterize the refractive index change in optical fibers induced by CO_2 laser irradiation,

4. Develop LPFG-based chemical sensors for various applications.

1.3. THESIS OVERVIEW

This thesis focuses on fabrication of high-performance LPFGs using a CO_2 laser and study of their high temperature performance. Applications of LPFGs as in-situ chemical sensors have also been explored in the form of bare gratings as well as nanomaterial-coated device. The thesis contains 6 Sections.

Section 2 focuses on the fabrication of LPFGs using CO_2 laser irradiation. The experimental setup for LPFG fabrication were described and discussed in detail in this section.

Section 3 concentrates on the high temperature performance of LPFG. It has been found that the thermal shock process could significantly improve the device's stability under high temperature.

Section 4 introduces a novel interferometric method to measure the refractive index modulation induced by laser irradiations. The measured value was used to guide the device design and fabrication.

In Section 5, two applications of LPFG will be demonstrated for chemical sensing. One was the measurement of refractive indices of different liquids using a bare LPFG, while the other was hydrogen concentration sensing under high temperatures using

Palladium coated LPFGs. The sensitivity, response time, stability and repeatability of these LPFG-based sensors were assessed based on the experimental data.

The conclusions and future work are summarized in Section 6.

2. FABRICATION AND BASIC TRANSMISSION CHARACTERISTICS

2.1. FABRICATION

The technique used to inscribe LPFGs is based on CO_2 laser exposure induced refractive index changes inside an optical fiber. Figures 2.1 and 2.2 show the schematic and photograph of the CO_2 laser base LPFG fabrication system, respectively. The LPFG inscription method used is similar to that described in Ref. 10 and Ref. 11. As shown in Fig. 2.1, a CO_2 laser (SYNRAD, Inc.) with a free space wavelength of 10.6μm and a maximum output power of 20W was used in the system. A ZnSe cylindrical lens with a focal length of 50mm was used to shape the CO_2 laser beam into a narrow line with a linewidth of 220μm. The CO_2 laser is controlled by the computer through the laser controller to produce a desired power.

The optical fiber (Corning SMF-28) with its buffer stripped is placed on a three dimensional (3D) motorized translation stage controlled by a computer, providing the option of displacing the translation stage in unison so that the fiber can be precisely moved to the center of the laser beam. The focused laser beam was transversely loaded onto the single mode optical fiber. Controlled by a computer, the translation stage moves the fiber at fixed step for laser exposure, resulting in a periodic refractive index modulation in the fiber core. The output power and exposure time-trajectory of the CO_2 laser could be accurately adjusted by a laser controller through computer software. A microscope video camera was used to visualize the micro-displacement of the optical fiber while the fabrication process is activated.

During grating fabrication, a tunable laser (HP81642A) and an optical power meter (HP 81618A) were also used to monitor the grating transmission spectrum. As shown in Fig. 2.2, the tunable laser is coupled into one end of the fiber and the other end is connected to the power meter. The tunable laser was controlled by the computer to step from 1510 to 1640 nm and the transmitted power after the grating was detected by the optical power meter so that the LPFG spectrum could be recorded in real-time during its fabrication.

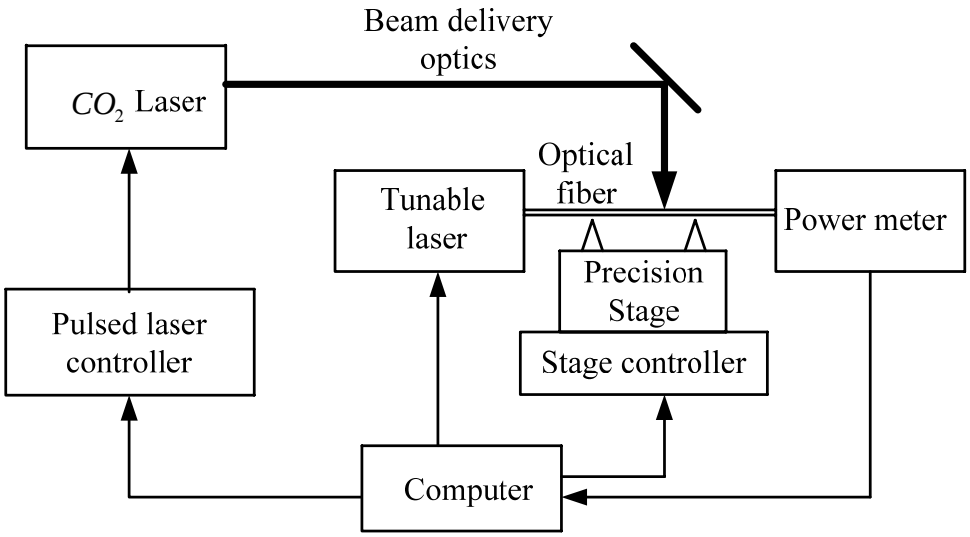

Figure 2.1 Schematic setup of the CO_2 laser based LPFG fabrication system

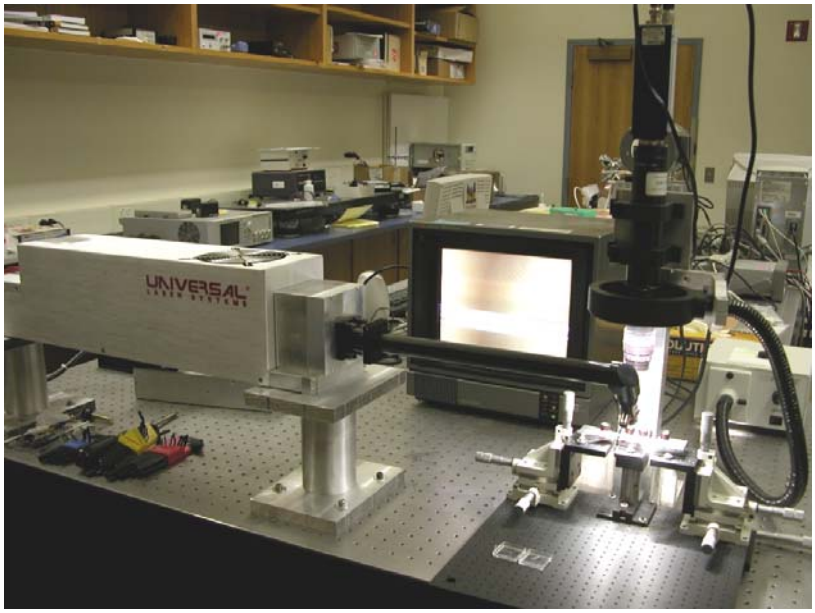

Figure 2.2 Photograph of LPFG fabrication system

2.2. TRANSMISSION CHARACTERISTICS

2.2.1. Typical Transmission Spectra. The transmission characteristics can be measured by the setup shown in Fig. 2.1. The tunable laser served as the light source at one end of the fiber and at the other end an optical power meter was used to detect the power transmitted through the grating. The wavelength stepping of the laser and the power detection of the power meter were coordinated by a computer. The typical transmission spectrum of the fabricated LPFG with a period of 535μm is shown in Fig. 2.3. The curve with black square dots is the resonance peak corresponding to the energy coupling from the fundamental core mode to the 5th cladding mode, while the curve with circles is the numerical simulation calculated based on an analytical modal following Ref. [34, 35]. The spectrum indicated a low loss (<1dB), a narrow Full-Width-at-Half-Maximum (FWHM <7nm) and a high resonance strength (>25dB) of the fabricated LPFG. Figure 2.3 shows that the measured transmission spectrum was in a good agreement with the simulated.

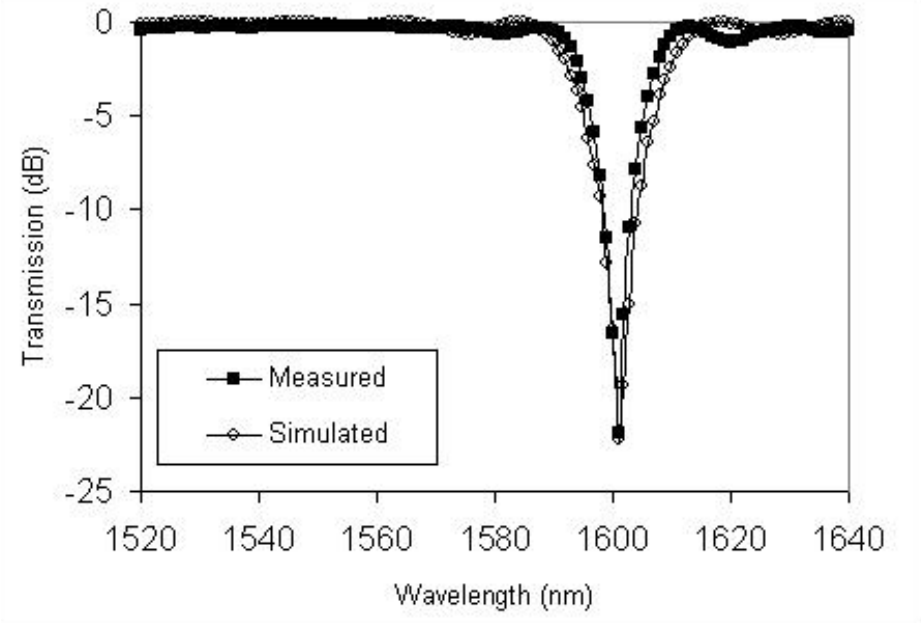

Figure 2.3 Measured and simulated transmission spectra of a LPFG with a period of 535μm

2.2.2. Typical Transmission Spectra with Different Periods. As shown in Fig. 2.4, by varying the grating period from 505 to 545μm, it is possible to effectively change the resonance wavelength of the LPFG from 1520 to 1640nm, which was mainly limited by the tuning range of the tunable laser. It is possible to further expand the resonance wavelength beyond the 1520 to 1640nm range. According to Eq. 1.2, since the effective refractive indices for both core mode and cladding mode are fixed after fabrication, the resonance wavelength is linearly proportional to the grating period. This linear relation was confirmed by the experiments as shown in Fig. 2.5.

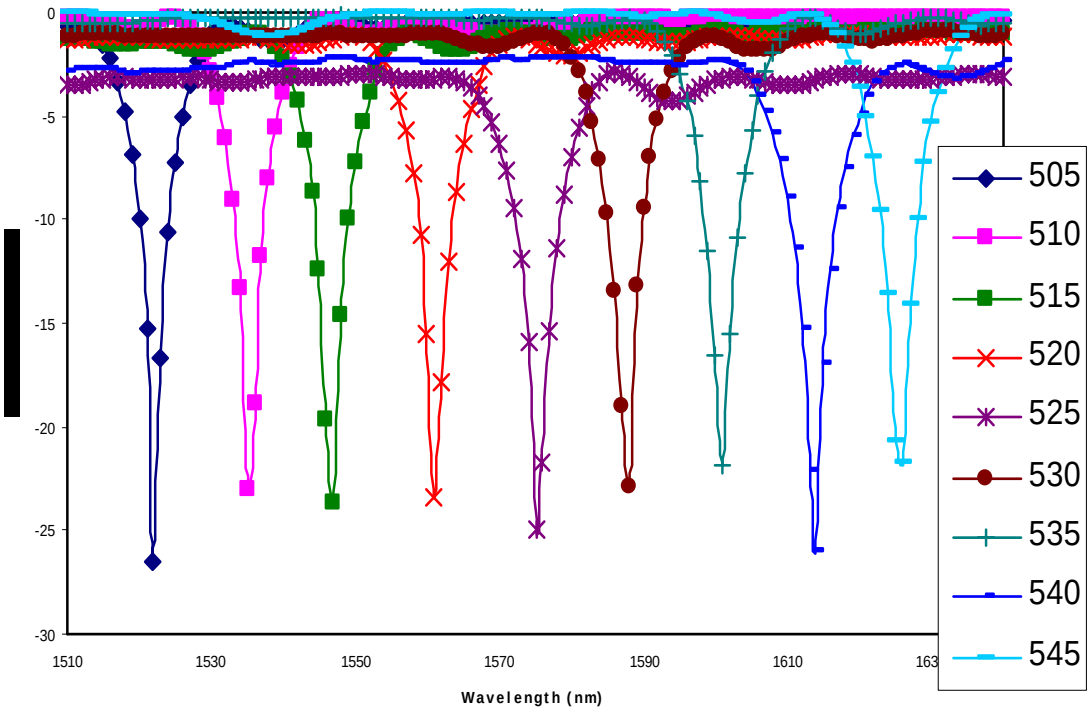

Figure 2.4 LPFG transmission spectra with different periods

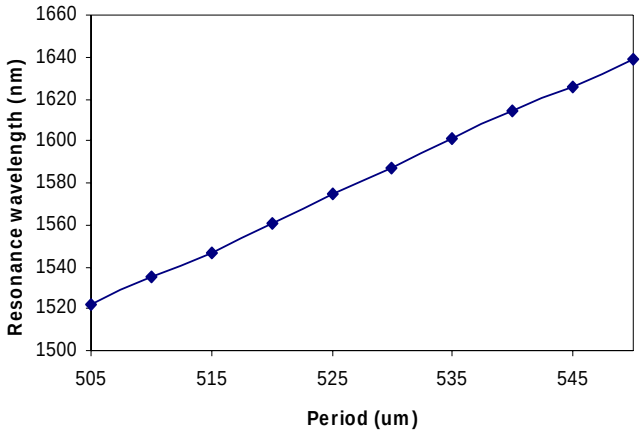

Figure 2.5 Resonance wavelength as a function of period

2.3. SUMMARY

In this section, the system and procedure for fabricating CO_2-laser-induced high-performance LPFGs were discussed. The typical transmission spectrum showed a low loss (<1dB), a narrow Full-Width-at-Half-Maximum (FWHM <7nm) and a high resonance strength (>25dB), which was adequate for most communication and sensing applications. The experimental data also confirmed that the resonance wavelength of CO_2-laser-induced LPFG varied linearly with the grating period. This linear relation can be used to guide the fabrication of LPFGs with any desired resonance wavelength.

3. HIGH TEMPERATURE PERFORMANCE AND IMPROVEMENT

3.1. HIGH TEMPERATURE SURVIVABILITY

To test the temperature survivability and sensitivity of the fabricated LPFGs, a LPFG was installed into an electric furnace and increased the temperature from 100°C to 800°C. The LPFGs used in the experience were fabricated with the same period of 500μm in Corning SMF-28 fiber. The temperature was held for one hour and measured the transmission spectrum of the LPFG at each 100°C increment as shown in Fig. 3.1. The grating transmission spectrum maintained the similar characteristics (e.g., strength and width) in all the temperatures except that the resonance wavelength of the LPFG moved to the long wavelength region when the temperature increased as shown in Fig. 3.1(a). Fig. 3.1(b) shows the resonant wavelength of the LPFG as a function of temperature. The test results clearly demonstrated that the LPFG successfully survived high temperatures up to 800°C. The results also indicated that the resonant wavelength was a linear function of temperature. This linear relation can be explained by the Eq. 1.2, where the grating period increased with the increase of temperature due to thermal expansion of the optical fiber.

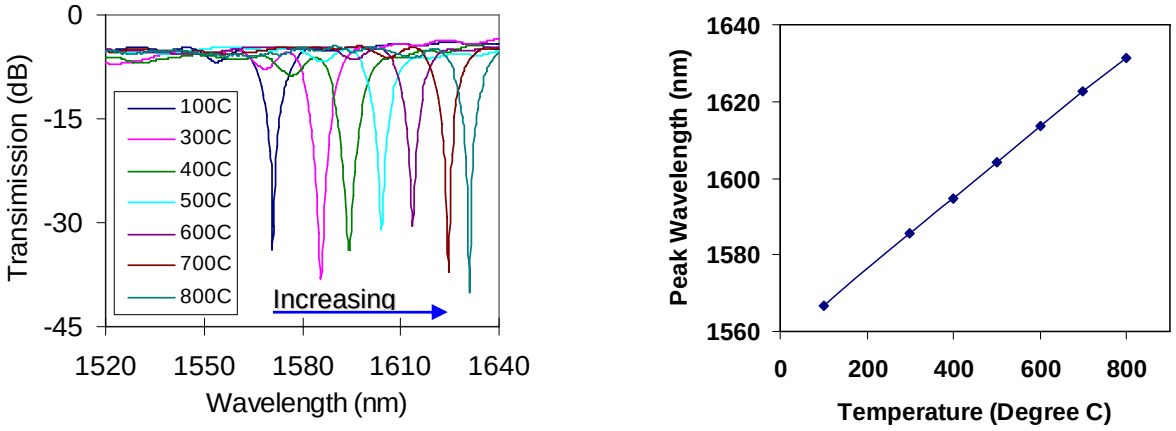

Figure 3.1 Test of LPFG at various temperatures (a) LPFG transmission spectra at different temperatures (b) resonance wavelength as a function of temperature

3.2. THERMO STABILITY AND IMPROVEMENT

3.2.1. Annealing. The stability of the LPFG is a concern when it is designed and fabricated for high temperature applications. It is highly desired that the resonance peak of the grating does not drift when the grating is exposed to a high temperature environment for a long period of time. However, due to the fact that the refractive index change is caused by thermal treatment and the inevitable thermal relaxation of the treated glass, it is expected that the resonance wavelength will have a non-reversible drift, especially in a high temperature environment.

To evaluate the thermal stability of the fabricated LPFG, a CO_2 laser fabricated LPFG was placed in electric furniture at a temperature of 550ºC. One end of the fiber was fixed to the test chamber (a ¼ inch stainless steel tube) while the other one was set loose so that the thermal expansion of the container itself would not affect the LPFG. As shown in Fig. 3.2, the lower curve with circle is the resonance wavelength as a function of time. A wavelength shift of 25.3nm after 200 hours was observed. It can also be seen that the wavelength change was faster at the beginning and getting slower as the experiment went along, indicating that the thermal stability of the LPFG improved after annealing. However, the improvement was slow and would take a long time to stabilize.

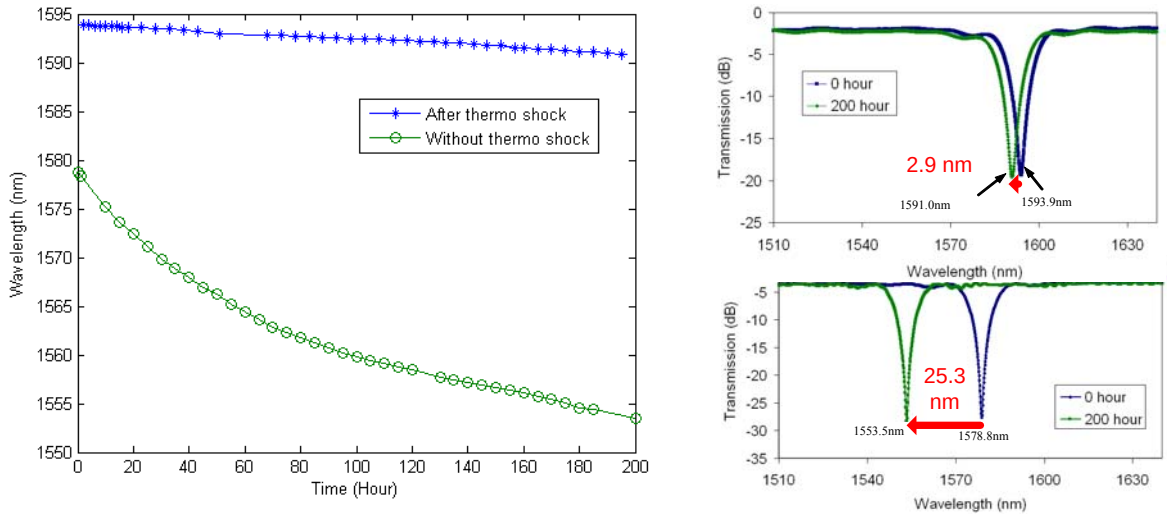

Figure 3.2 Thermo stability tests and improvement

3.2.2. Thermal Shock. In the second experiment, a LPFG was heated up to 700ºC for 2 hours, and then, cooled it down to 550ºC and maintained for 200 hours. As shown in Fig. 3.2 (the upper curve), the resonant wavelength still shows a continuous drift towards a shorter wavelength but with a much smaller shift of 2.9nm after 200 hours annealing. The experiment indicates that thermal shock indeed improved the thermo stability of LPFG at high temperatures. To better understand the reason under this thermal shock phenomenon, it is necessary to go to the material fundamentals and the micro structure performance of the quiz. It is believed to be an issue in the future research.

3.3. SUMMARY

In this section, the performance of LPFG under high temperatures has been evaluated experimentally. The LPFG successfully survived high temperatures up to 800ºC without performance degradation. Not surprisingly, it was also found that the resonance wavelength of the as-fabricated LPFG has a large non-reversible drift when it was subjected to a long-term high temperature annealing test. However, it has also been found that the thermal drift could be significantly reduced by a simple thermal shock process at an elevated temperature. The improved thermal stability of LPFG is of great importance for applying the device to long-term monitoring in a high temperature environment.

4. REFRACTIVE INDEX MODULATION MEASUREMENT

4.1. MEASUREMENT THEORY

4.1.1. CO_2 Laser Exposure Profile Approximation. It has been explained that the change of refractive index comes mainly from stress relaxation effect of thermal shocks [10, 11]. The amount of refractive index modulation inside a fiber core is one of the most critical variables that determine the transmission characteristic of an LPFG. Accurate knowledge of the CO_2 laser irradiation caused refractive index changes can thus help adjust the laser pulse parameters such as the power and pulse duration to fabricate LPFGs with desired performance.

As shown in the inset of Fig. 4.1, the upper figure shows the refractive index distribution profile of laser exposure. Assuming that the change of RI in fiber core is

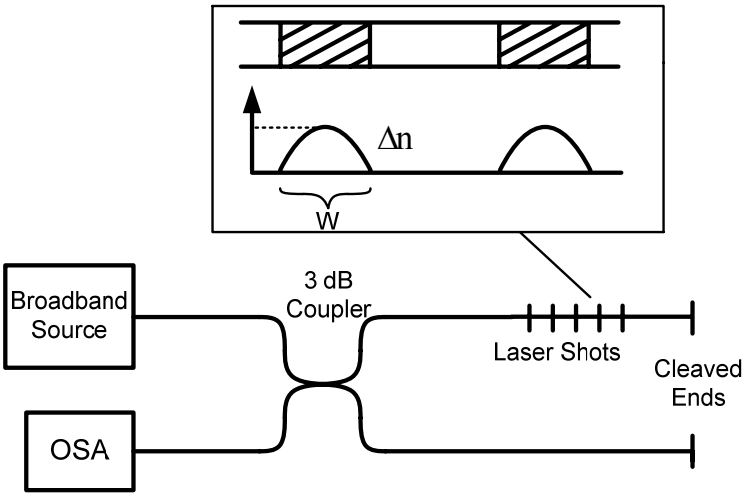

Figure 4.1 Setup schematic of measurement

sinusoid-distributed and the highest RI change Δn happens at the center of laser-exposed fiber area, the change of optical path (OP) induced by one laser shot could be expressed as

$$\Delta OP = \int_0^W \Delta n \sin(\frac{x}{W}\pi)dx \tag{4.1}$$

where W represents the beam width of the beam shaped line width of laser exposure. Solving the integral in Eq.1, it will be

$$\Delta OP = \frac{2W\Delta n}{\pi} \tag{4.2}$$

4.1.2. Measurement Principle. The peak refractive index change Δn can be measured using a white light fiber optic Michelson interferometer as schematically shown in Fig. 4.2. A 3dB coupler splits the light from a broadband source into the two fiber arms with cleaved endfaces. The reflections from the two endfaces form the interference signal that is recorded by an optical spectrum analyzer (OSA). One fiber is kept undisturbed to serve as the reference path. The other fiber, with its cladding stripped, is placed on a computer-controlled three-dimensional translation stage to be exposed to CO_2 laser irradiation at different locations.

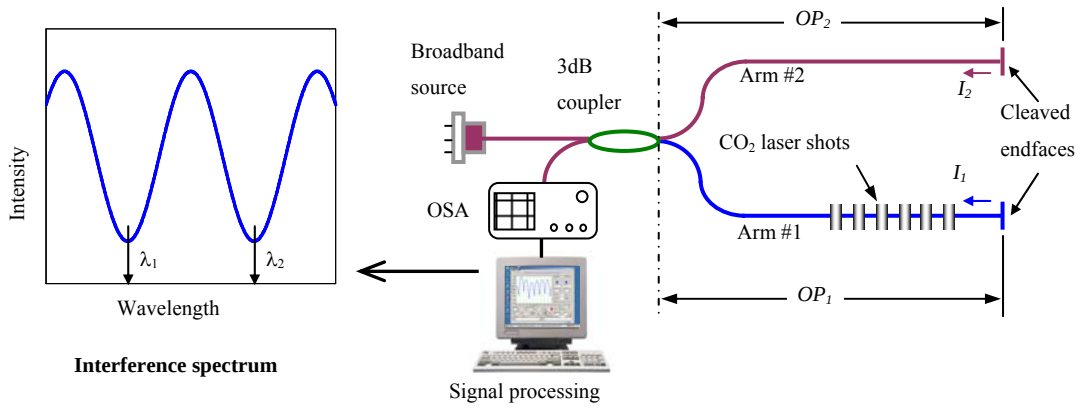

Figure 4.2 Fiber optic Michelson interferometer to measure refractive index modulation

Assuming that the two reflected lights from the cleaved fiber endfaces have the intensities of I_1 and I_2, respectively, the interference signal I generated by these two reflections as collected by OSA is given by:

$$I = I_1 + I_2 + 2\sqrt{I_1 I_2}\sin\left(\frac{4\pi}{\lambda}(OP_1 - OP_2)\right) \tag{4.3}$$

where OP_1 and OP_2 are the forward propagation optical paths (defined as the product of the length and refractive index of the core) of the two arms, respectively. The optical path difference (*OPD*) between the two fiber arms is given by $OPD = OP_1 - OP_2$.

As shown in Fig. 4.2, the two adjacent valleys at λ_1 and λ_2 in the interference spectrum have a phase difference of 2π, that is:

$$\left(\frac{4\pi}{\lambda_1}OPD\right) - \left(\frac{4\pi}{\lambda_2}OPD\right) = 2\pi \tag{4.4}$$

Therefore, the *OPD* between the two arms can be calculated using the following equation:

$$OPD = \frac{\lambda_1\lambda_2}{2(\lambda_1 - \lambda_2)} \tag{4.5}$$

It is further assumed that the physical length of the fiber does not vary before and after laser irradiation. Therefore, the change of the *OPD* between two fiber arms is mainly caused by the laser irradiation induced refractive index change inside the fiber core.

For multiple-point laser irradiations (with the same laser conditions) at different locations, the accumulated change in *OPD* is given by

$$OPD_{after} - OPD_{before} = m\Delta OP_{Single} \tag{4.6}$$

where *m* is the number of laser irradiation points on the optical fiber, OPD_{before} and OPD_{after} are the optical path differences before and after the *m*-point CO_2 laser irradiations, and ΔOP_{Single} is the optical path change induce by single laser shot, denoted in Eq. 4.2. The refractive index modulation Δn can thus be determined based on Eq. 4.6.

$$\Delta n = \frac{\pi(OPD_{after} - OPD_{before})}{2mW} \tag{4.7}$$

4.2. EXPERIMENT

A fiber optic Michelson interferometer was constructed based on Fig. 4.2. The fiber used in the experiment was Corning SMF-28 single mode fiber. The two fibers were cleaved simultaneously to make the initial OPD as small as possible. The broadband source used was made by multiplexing a C-band and an L-band Erbium doped fiber ASE (amplified spontaneous emission) sources, which covered the spectral range from 1530 to 1610nm.

The two fiber arms were set relaxed on an air-isolated optical table and aligned in parallel to allow the initial interference spectrum to be recorded by an OSA (HP 70952B). Then one fiber was mounted onto the 3D translation stage and exposed to 150 shots of CO_2 laser irradiations at different locations. The exposure power and duration were set as the same as used in grating fabrication. It is important to note that the distance between two adjacent irradiations was set randomly to avoid grating effect in the interference spectrum. After laser exposures, the interference fringe was recorded again by removing the fiber from the stage and placing the two fibers on the optical table at their marked positions where the initial interference spectrum was taken. Then the process was repeated to increase the number of laser exposure points the same fiber.

4.3. RESULTS AND DISCUSSIONS

Figure 4.3 plots the results of this experiment, in which Fig. 4.3(a) shows the initial interference spectrum and those after 150, 300, and 450 points irradiations. Since each laser exposure induced a small amount of power loss, the amplitude of the interference signal was reduced as the number of laser exposures increased. The spectral separation of the two adjacent interference valleys decreased with the number of laser exposures, indicating the increase of the OPD. Figure 4.3(b) plots the OPD as a function of the number of laser exposures. The measured data points fit nicely into a line as predicted. It has been obtained that each laser shot brings a 36.676nm change in OPD. Given the W=220μm which is the beam width of the laser, the peak index modulation Δn was calculated to be 2.6×10^{-4} based on the slope of the line.

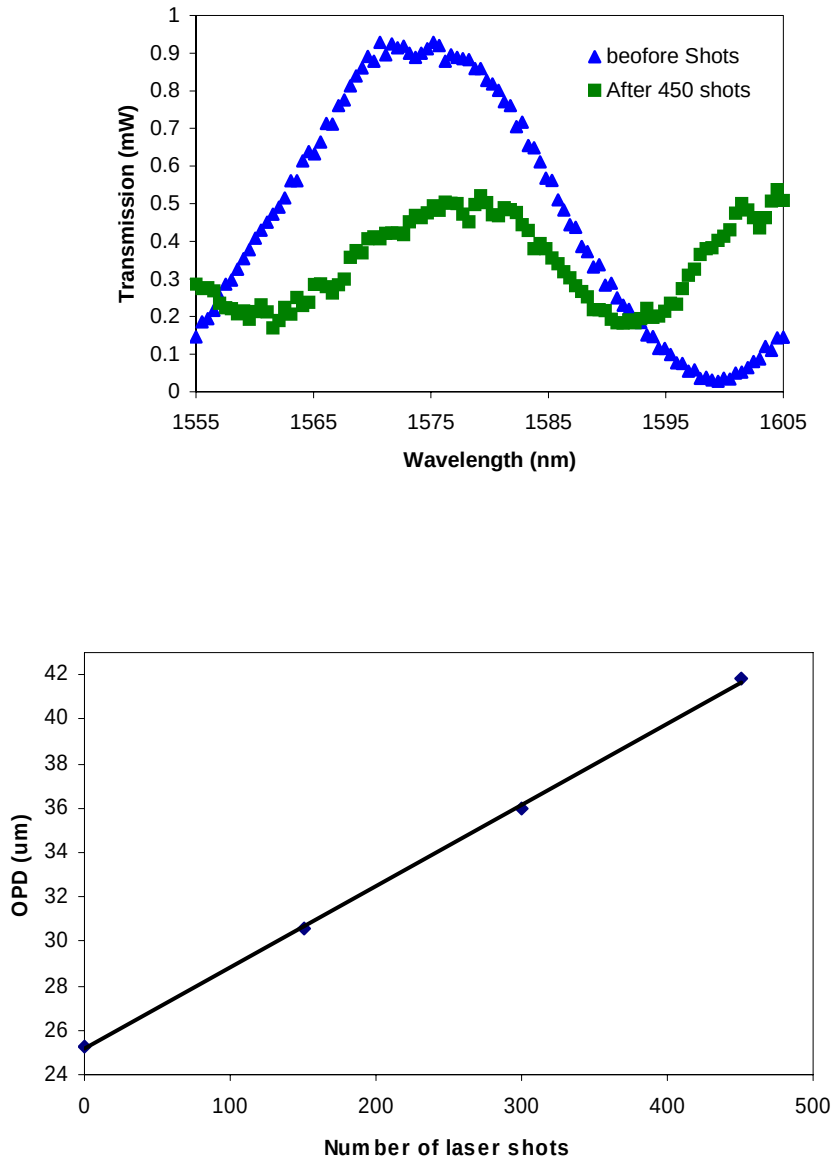

Figure 4.3 Results of refractive index modulation measurement; (a) interference spectra and polynomial fitted curves of various number of laser irradiations; (b) optical path difference as a function of the number of laser exposures

The transmission spectrum from modeling with this index modulation value fits nicely with the LPFG spectrum fabricated with the same laser pulse parameters as shown in Fig. 2.3.

4.4. SUMMARY

In conclusion, an interferometric method was developed to measure the refractive index change induced by CO_2 laser irradiation. In this method, the laser-induced refractive index change was assumed to have a sinusoid distribution and each of the laser shot would bring an OPD change. The OPD was measured to be 2.6×10^{-4} based on the phase shift of the interference fringe. The measured refractive index modulation was used to simulate the LPFG transmission spectrum. The simulation was in a good agreement with the measured transmission spectrum.

5. APPLICATIONS

5.1. AMBIENT REFRACTIVE INDEX MEASUREMENT

Because the phase matching condition depends on the effective indices of the coupled cladding modes, which rely on the difference between the refractive index of the cladding and that of the medium surrounding the cladding, the resonance wavelengths of the LPFG show a dependence upon the refractive index of the medium surrounding cladding. LPFGs can thus be used to monitor the refractive index of the surrounding medium. To investigate the effect of refractive index of the surrounding medium on the resonance wavelength, the LPFG was placed in the air (refractive index =1), water (refractive index = 1.33), acetone (refractive index = 1.3590) and isopropanol (refractive index = 1.3776) and measured the transmission spectrum of the LPFG, respectively. As shown in Fig. 5.1, the LPFG, fabricated with a period of 530μm using a Corning

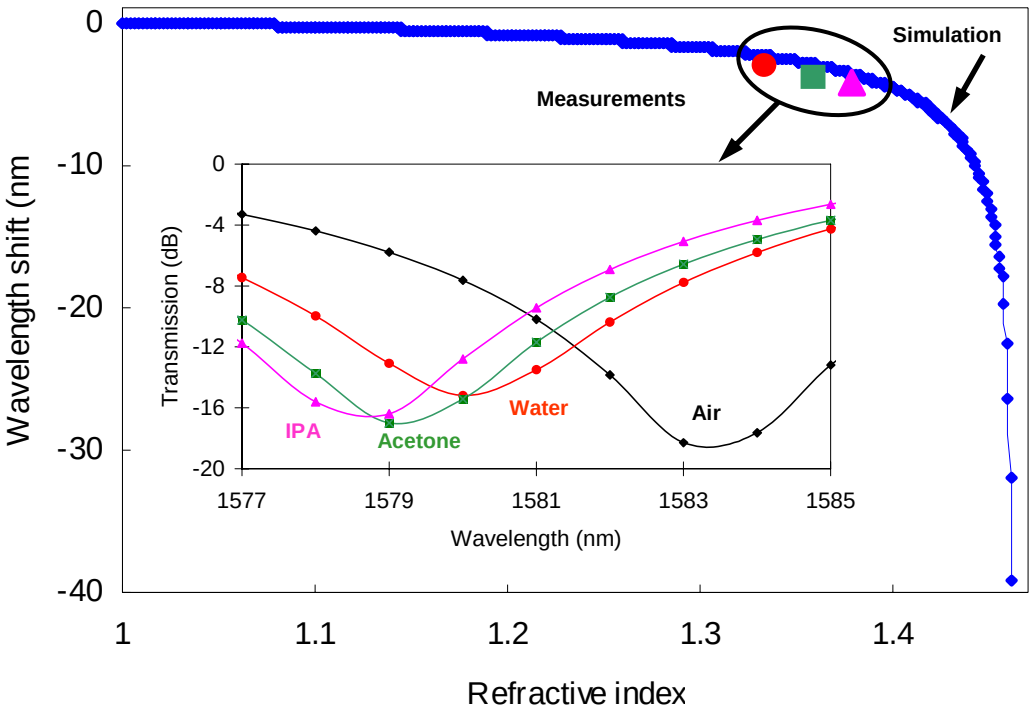

Figure 5.1 LPFG in response to ambient refractive index changes

SMF-28 fiber, had a resonance wavelength of 1583.23nm in air. Its resonance wavelength shifted to 3.0229, 4.0019, and 4.3783nm when placed in water, acetone, and isopropanol, respectively. In general, the resonant wavelength shifted towards the short wavelength region as the environmental refractive index increased.

Figure 5.1 also plots the simulated resonance wavelength shift, with respect to that in air, as a function of the refractive index of the surrounding environment. The three measurement data points were charted on the simulated curve and found that the measured data were in a good agreement with the numerical simulations.

5.2. PALLADIUM COATED LPFG FOR HYDROGEN SENSING

5.2.1. Introduction. Considered as a clean and renewable energy source, hydrogen has become a promising alternative to fossil fuels to solve the energy crisis and pollution problems. Consequently, in-situ monitoring hydrogen concentration has become important for the purposes of process control in hydrogen production and safety guard in hydrogen applications. In the last two decades, great efforts have been devoted into the development and commercialization of electrical type hydrogen sensors. Even though some of them exhibited high sensitivity and fast response time, a main drawback of electrical type sensors is that the use of electricity may lead sparks at the sensing point. As an alternative, optical sensors seem to be more attractive due to the lack of sparking possibilities. Moreover, most optical hydrogen sensors operate in a non-contact mode and can be deployed into regions where common electrical sensors are difficult to reach, especially when an optical fiber is used to transmit the signal [36]. To perform hydrogen sensing, many of these optical sensors use specially designed sensing materials that selectively interact with hydrogen molecules to generate an optical signal [37, 38].

5.2.2. Principle of Operation. The hydrogen sensor designed in this work selected palladium (Pd) as the sensing material [39]. When Pd is exposed to hydrogen, hydrogen dissociates into two hydrogen atoms at the Pd surface with an efficient rate. The hydrogen atoms then diffuse into the palladium, resulting in the formation of palladium hydride (PdH). The hydration of Pd is also reversible. When the hydrogen concentration in the environment reduces, the Pd releases the adsorbed hydrogen. The

hydration leads to an increase in the lattice parameters and consequently a decrease in the volume density of free electrons. As a result, the complex refractive index of the Pd changes, which can be used to monitor the hydrogen concentration in the environment.

The unique hydrogen related optical property of Pd can be used to develop a hydrogen sensor when integrated with a photonic device, such as the LPFG described in this thesis. The concept is to coat a thin layer of Pd film on a LPFG. Upon exposure to hydrogen, the coated Pd film changes its refractive index and correspondingly the mode coupling condition, resulting in a shift of the resonance wavelength of the grating. Therefore, by monitoring the resonance wavelength shift, the change of the hydrogen concentration can be accurately detected [40].

5.2.3. Experiment Setup. The nanosized Pd thin layer was deposited on LPFG by magnetron sputter deposition. During the deposition, the fiber was rotated periodically in order to prepare the thin film coating with relatively uniform thickness.

The schematic of hydrogen concentration sensing system is shown in Fig. 5.2.

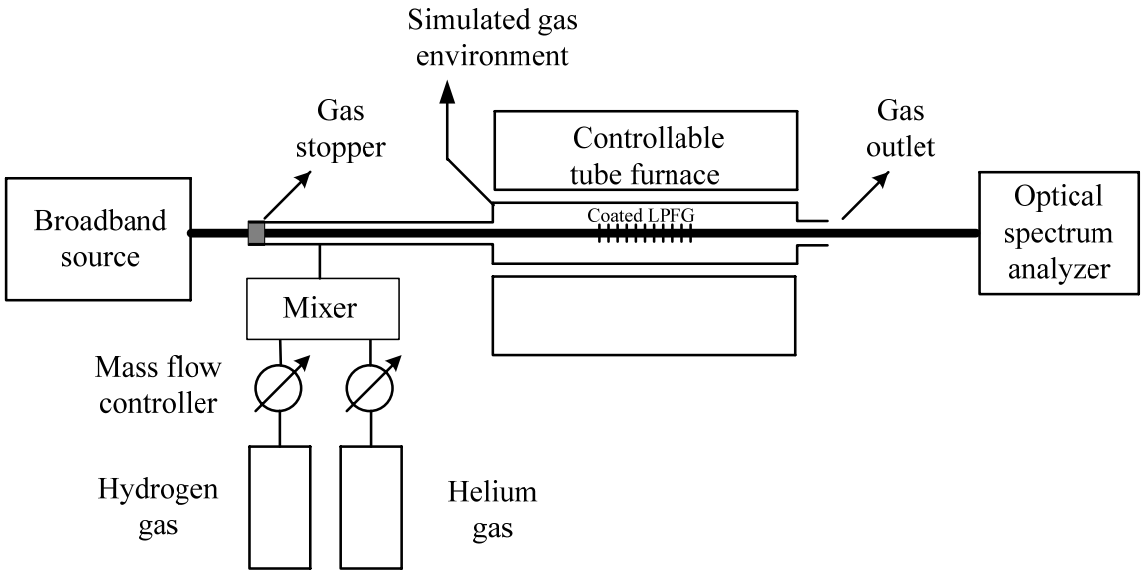

Figure 5.2 Schematic of Pd-LPFG in-situ measurement for hydrogen concentration sensing

The Pd coated LPFG was placed in a 1/8-inch stainless steel tube. To simulate the actual application environment, two cylindrical gas tanks were connected to the stainless steel tube through a mixer. One is filled with hydrogen gas, while the other is helium gas. The gas flow rates of these two gases can be controlled individually by adjusting the mass flow controllers to obtain the desired concentration of hydrogen inside the stainless steel tube. The stainless steel tube was hosted inside an electric tubular furnace, by which the environmental temperature can be controlled. During sensor installation, one end of the Pd-coated LPFG sensor was fixed to the stainless steel tube by a gas stopper, while the other end was set free to eliminate stress. The two ends of the fiber were connected to a broadband optical source and an optical spectrum analyzer (OSA), respectively. The resolution bandwidth was set 2nm, while the number of the points taken by OSA within certain wavelength range was set 1000 for each scan. The OSA was connected to a computer, where the transmission spectrum of the LPFG was recorded and analyzed.

5.2.4. Result and Discussion. Figure 5.3 shows a scanning electronic micrograph (SEM) of the Pd-coated LPFG (Pd-LPFG), indicating a thin layer of uniform, defect-free Pd film has been successfully coated on the LPFG. The high magnification SEM image of the film (Fig. 5.3.b) suggested that the Pd film had a nanostructure with a grain size distribution in the range of 20-30nm. It is preferred that the Pd coating remains in this nanostructure as it facilitates the speed of hydrogen adsorption and desorption. The thickness of the coating can be varied by change the duration of sputtering. In general, a thick coating results in high detection sensitivity. However, thick film will also reduce the speed of detection. Therefore, there is a tradeoff between the speed and sensitivity.

Prior to the test of the Pd-LPFG in response to hydrogen, the temperature dependence of the sensor was characterized. In the work, the shift of wavelength was found to be 35 pm/°C. The Pd-LPFG sensor was then tested in the temperatures ranging from 30 to 250°C under various hydrogen concentrations. To minimize the noise influences, each measured transmission spectrum was first partially fitted by a 4-th order polynomial series. The resonance wavelength was then calculated as the tuning point of the fitted polynomial.

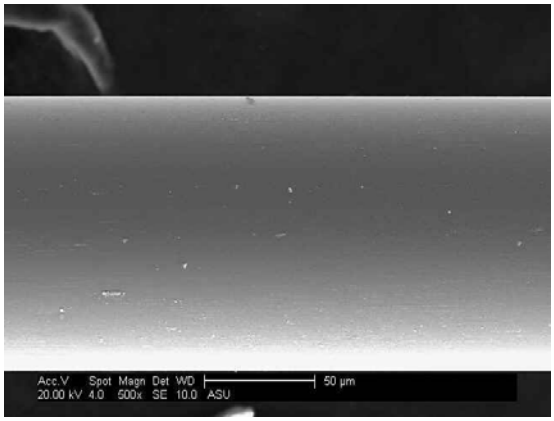

(a)

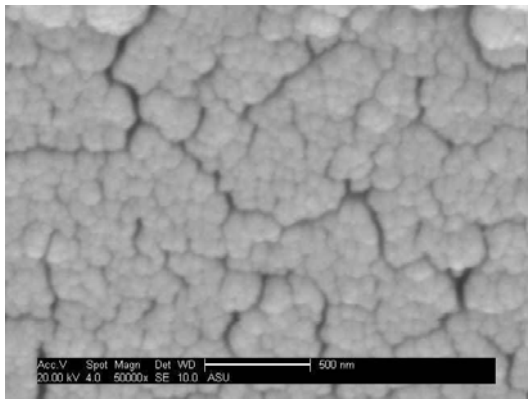

(b)

Figure 5.3 SEM image of Pd-coated LPFG (a) 500x magnification (b) 50000x magnification

The transmission spectrums of Pd-LPFG in helium and 8% hydrogen at various temperatures are shown in Fig. 5.4, where the resonance wavelength clearly shifted towards the short wavelength region (blue shift) indicating the increase of Pd refractive index as a result of hydrogen adsorption into the thin film. Comparing the sensor response at various temperatures, it has been found that the amount of resonance wavelength shift highly depended on the temperature. As the temperature went up, the amount of blue shift decreased in response to 8% hydrogen concentration change. At

room temperature, 8% hydrogen induced 4.2nm of shift in resonance wavelength. While at 200°C, the same 8% hydrogen only caused about 0.1nm shift.

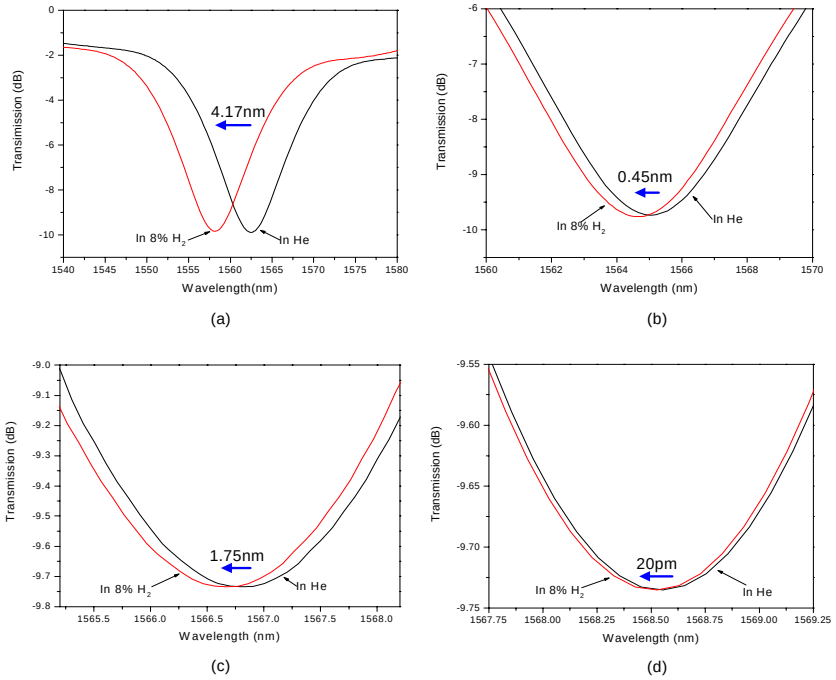

Figure 5.4 Spectrum of LPFG coated with Pd in 8% H_2 and H_2 free atmosphere at (a) room temperature (b) 100°C (c) 150°C (d) 200°C

The dependence of resonance wavelength shift as a function of hydrogen concentration at different temperatures is shown in Fig. 5.5. In general, it has been found that the amount of blue shift was almost linearly proportional to the hydrogen concentration up to 16%. However, the sensor response decreased significantly as the temperature increased. This can be explained by the fact that the hydrogen adsorption into the film reduces as the temperature increases. Even at 200°C, 4% hydrogen concentration increment resulted in a10pm shift in the resonance wavelength, which was still detectable using the existing system. However, when testing the sensor at 250°C, the amount of hydrogen dissolved into Pd was too low to cause any observable wavelength

shift in the hydrogen concentration up to 16%. In conclusion, the tests successfully proved that Pd-LPFG sensor was working properly as expected in the temperature range from 25°C to 200°C.

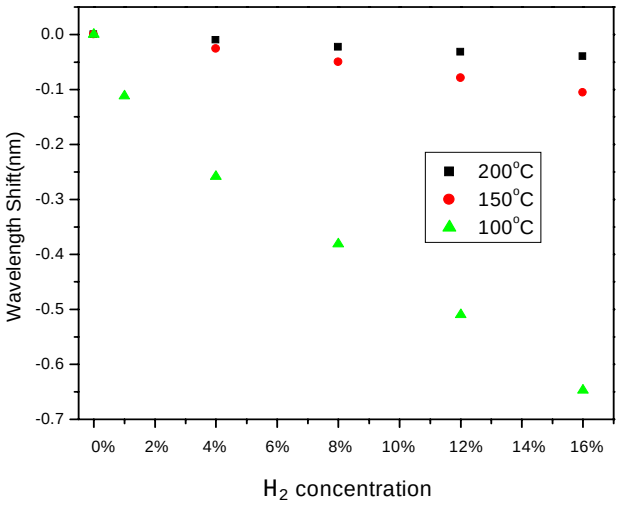

Figure 5.5 Wavelength shift as a function of H_2 concentration at various temperatures

The temporal characteristic of the Pd-LPFG in response to the hydrogen was also experimentally tested. Figure 5.6 shows the response and recovery time of Pd-LPFG when the sensor was exposed to 4% hydrogen at room temperature and 100°C, respectively. At each temperature, the response time to 4% hydrogen was less than one minute. The uptake time at 100°C was slightly shorter than that at room temperature. Compared to the hydrogen uptake process, the recovery time was much longer. At room temperature, it took about 5 minutes to shift back to the 90% of the original position in pure helium, and about 14 minutes to reach the completely stabilized point. It is worth noting that the response and recovery times also included the time required for the experimental setup to stabilize. At 100°C, the recovery time was much shorter than the case under room temperature. It took about 1 minute for the sensor recover to the 90% of its original value, and less than 5 minute to reach stabilization. The shorter response and

recovery times of the sensor at a higher temperature can be explained by that fact that the adsorption and desorption of hydrogen are much fast at an elevated temperature as predicted by the thermal dynamics.

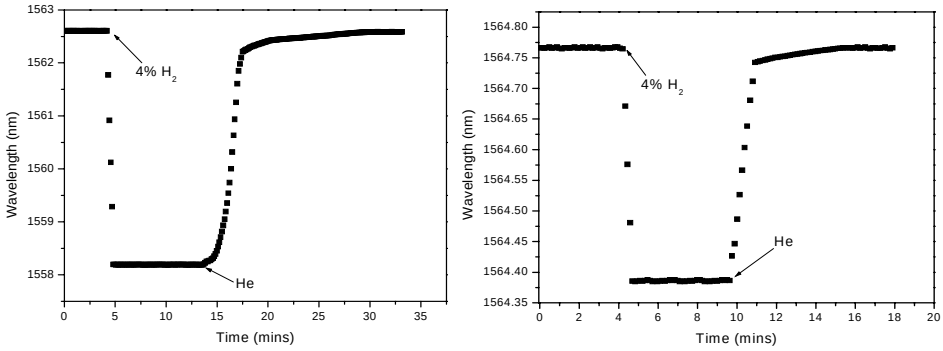

(a) (b)

Figure 5.6 Response time and recovery time of LPFG in 4% H_2 at (a) room temperature (b) 100^{o}C

The repeatability of the Pd-LPFG sensor in response to hydrogen was also experimentally evaluated at room temperature and 100°C, respectively, with the results shown in Fig. 5.7. In each test, the sensor was exposed to 4% hydrogen and recovered by pure helium for 5 cycles. The results indicated no observable difference in either the response time or the amount of wavelength shifts in different cycles, implying that the whole absorption and desorption process was repeatable within accuracy of instruments.

5.3. SUMMARY

In this section, two applications of LPFG have been demonstrated. The first application focused on the evaluation of the sensing capability of a bare LPFG towards the ambient refractive index change. the experimental results showed a good agreement with the simulation data. The second application was concentrated on development of a

Pd-coated LPFG sensor for in-situ monitoring hydrogen concentrations at various temperatures. The sensitivity, response time, temperature dependence, and repeatability

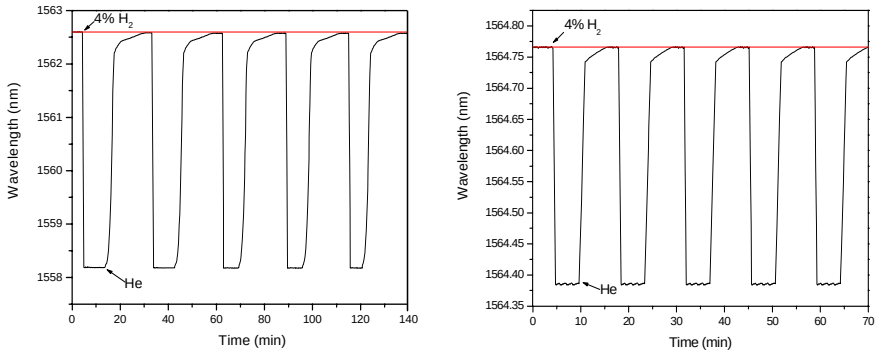

(a) (b)

Figure 5.7 Repeatability test of Pd-LPFG at (a) room temperature (b) 100^{o}C

have been systematically evaluated. In general, it has been proved that the Pd-coated LPFG could be used to sensitively monitor the hydrogen concentration in the temperature range of 25°C to 200°C.

6. CONCLUSION

Long period fiber gratings have many unique advantages such as small insertion loss, low retro-reflection, good sensory property and low cost fabrication. People have found many applications in optical fiber communications and in optical fiber sensors. Recently, the potential applications of fiber sensors in high temperature environment have attracted considerable interests. Optical fibers have a proven reputation of being high temperature-tolerant due to its glass nature. In addition, optical fiber sensors possess a key advantage over electronic sensors. It is naturally free from electrical sparks which might lead to a serious explosion under extreme conditions. Therefore, it is a natural path to extend the sensing capabilities of LPFGs to meet the ever increasing needs for sensors that can survive high temperature harsh environment.

Most of the existing LPFGs are made by UV laser irradiation. However, the UV induced refractive index changes are found difficult to survive high temperatures. Nowadays, CO_2 lasers have been used for fabricating LPFGs. One of the greatest advantages of using the CO_2 laser irradiation technique is that it is simple and flexible to use but still providing a high thermal stability. The main objective of this thesis is to implement a CO_2-laser-irradiation-based method to fabricate high performance temperature tolerant LPFGs.

The thesis work included the establishment of a computer controlled fabrication system with in-situ signal monitoring capability, the characterization of the fabricated LPFGs, high temperature survival ability and stability test in together with its improvement , the measurement of CO_2 Laser induced refractive index change and LPFG-based chemical sensors for various applications. The major conclusions of the thesis work are summarized as following:

The system and procedure for fabricating CO_2-laser-induced high-performance LPFGs were discussed. The typical transmission spectrum showed a low loss (<1dB), a narrow Full-Width-at-Half-Maximum (FWHM <7nm) and a high resonance strength (>25dB), which was adequate for most communication and sensing applications. The experimental data also confirmed that the resonance wavelength of CO_2-laser-induced

LPFG varied linearly with the grating period. This linear relation can be used to guide the fabrication of LPFGs with any desired resonance wavelength.

The performance of LPFG under high temperatures has been evaluated experimentally. The LPFG successfully survived high temperatures up to 800ºC without performance degradation. It has been found that the resonance wavelength of the as-fabricated LPFG has a large non-reversible drift when it was subjected to a long-term high temperature annealing test. However, it has also been found that the thermal drift could be significantly reduced by a simple thermal shock process at an elevated temperature. The improved thermal stability of LPFG is of great importance for applying the device to long-term monitoring in a high temperature environment.

An interferometric method to measure the refractive index change induced by CO_2 laser irradiation has been developed. In this method, the laser-induced refractive index change was assumed to have a sinusoid distribution and each of the laser shot would bring an OPD change. The OPD was measured to be 2.6×10^{-4} based on the phase shift of the interference fringe. The measured refractive index modulation was used to simulate the LPFG transmission spectrum. The simulation was in a good agreement with the measured transmission spectrum.

After all, two applications of LPFG have been demonstrated. The first application focused on the evaluation of the sensing capability of a bare LPFG towards the ambient refractive index change. The experimental results showed a good agreement with the simulation data. The second application was concentrated on development of a Pd-coated LPFG sensor for in-situ monitoring hydrogen concentrations at various temperatures. The sensitivity, response time, temperature dependence, and repeatability have been systematically evaluated. In general, it has been proved that the Pd-coated LPFG could be used to sensitively monitor the hydrogen concentration in the temperature range of 25°C to 200°C.

Till now, the high temperature chemical sensing capability has been well proven. The next step will be establishing a more detailed model consisting of the outside layer modes, which will make it possible to find out the quantities' relation between outside layer refractive index change and the resonance wavelength shift. Meanwhile the multi layer model will help understand the absorption and desportion process better. This

analysis in together with the future experimental investigations will eventually result in high performance chemical sensors to meet the urgent needs in various important applications in defense, energy, environmental and biomedical areas.

BIBLIOGRAPHY

[1] L. Eldada, "Optical communication components," *Rev. Sci. Instr.*, vol. 75, pp. 575–593, Mar. 2004.

[2] Y. -G. Han, S. Kim, and S. Lee, "Flexibly tunable multichannel filter and bandpass filter based on long-period fiber gratings," *Opt. Express* 12, 1902-1907, 2004.

[3] H. An, B. Ashton, and S. Fleming, "Long-period-grating-assisted optical add-drop filter based on mismatched twin-core photosensitive-cladding fiber," *Opt. Lett.* 29, 343-345, 2004.

[4] B. J. Eggleton, R. E. Slusher, J. B. Judkins, J. B. Stark, and A. M. Vengsarkar, "All-optical switching in long-period fiber gratings," *Opt. Lett.* 22, 883-885, 1997.

[5] E. Udd, ed., Fiber Optic Sensors: An Introduction for Scientists and Engineers. *New York: John Wiley and Sons*, 1991.

[6] A. Othonos and K. Kalli, Fiber Bragg Gratings: Fundamentals and Applications in Telecommunications and Sensing. *Boston: Artech House*, 1999.

[7] A. M. Vengsarkar, P. J. Lemaire, J. B. Judkins, V. Bhatia, T. Erdogan, and J. E. Sipe, "Long-period fiber gratings as band-rejection filters," *J. Lightwave Technol.*, vol. 14, pp. 58–65, Jan. 1996.

[8] Q. Li, C.-H. Lin, A. A. Au, and H. P. Lee, "Compact all-fibre on-line power monitor via core-to-cladding mode coupling," *Electron. Lett.*, vol. 38, pp. 1013–1015, Aug. 29, 2002.

[9] D. B. Stegall and T. Erdogan, "Dispersion control with use of long-period fiber gratings," *J. Opt. Soc. Am. A*, vol. 17, pp. 304–312, Feb. 2000.

[10] D.D. Davis, T.K. Gaylord, E.N. Glytsis, S.G. Kosinski, S.C. Mettler and A.M. Vengsarkar, "Long-period fibre grating fabrication with focused CO_2 laser pulses," *Electron. Lett.*, 34, pp. 302-303, 1998.

[11] Yun-Jiang Rao, Yi-Ping Wang, Zeng-Ling Ran, and Tao Zhu, "Novel Fiber-Optic Sensors Based on Long-Period Fiber Gratings Written by High-Frequency CO_2 Laser Pulses," *J. Lightwave Techno.* 21, pp. 1320-1327, 2003.

[12] D.D. Davis, T.K. Gaylord, E.N. Glytsis and S.C. Mettler, "Very-high-temperature stable CO_2-laser-induced long-period fibre gratings," *Electron. Letter.* 35, pp. 740-742, 1999.

[13] S. Nam, C. Zhan, J. Lee, C. Hahn, K. Reichard, P. Ruffin, K. -L. Deng, and S. Yin, "Bend-insensitive ultra short long-period gratings by the electric arc method and their applications to harsh environment sensing and communication," *Opt. Express* 13, 731-737, 2005.

[14] S. G. Kosinksi and A. M. Vengsarkar, "Splicer-based long-period fiber gratings," in Optical Fiber Communication Conference, (Washington, D.C.), pp. 278–279, *Optical Society of America*, Feb. 1998.

[15] G. Humbert, A. Malki, S. Février, P. Roy, and D. Pagnoux, "Characterizations at high temperatures of long-period gratings written in germanium-free air silica microstructure fiber," *Opt. Lett.* 29, 38-40, 2004.

[16] Y. Kondo, K. Nouchi, T. Mitsuyu, M.Watanabe, P. G. Kazansky, and K. Hirao, "Fabrication of long-period fiber gratings by focused irradiation of infrared femtosecond laser pulses," *Opt. Lett.*, vol. 24, pp. 646–648, May 15, 1999.

[17] M. Fujimaki, Y. Ohki, J. L. Brebner, and S. Roorda, "Fabrication of long-periodoptical fiber gratings by use of ion implantation," *Opt. Lett.*, vol. 25, pp. 88–89, Jan.15, 2000.

[18] Y. Jeong, B. Yang, B. Lee, H. S. Seo, S. Choi, and K. Oh, "Electrically controllable long-period liquid crystal fiber gratings," *IEEE Photon. Technol. Lett.*, vol. 12, pp. 519–521, May 2000.

[19] S. Savin, J. F. Digonnet, G. S. Kino, and H. J. Shaw, "Tunable mechanically induced long-period fiber gratings," *Opt. Lett.*, vol. 25, pp. 710–712, May 15, 2000.

[20] T. Yokouchi, Y. Suzaki, K. Nakagawa, M. Yamauchi, M. Kimura, Y. Mizutani, S. Kimura, and S. Ejima, "Thermal tuning of mechanically induced long-period fiber grating," *Appl. Opt.* 44, 5024-5028, 2005.

[21] N. D. Rees, S. W. James, R. P. Tatam, and G. J. Ashwell, "Optical fiber long-period gratings with Langmuir—Blodgett thin-film overlays," *Opt. Lett.* 27, 686-688, 2002.

[22] X. Shu, L. Zhang, and I. B. and, "Sensitivity characteristics of long-period fiber gratings," *J. Lightwave Technol*., vol. 20, pp. 255–266, Feb. 2002.

[23] V. Bhatia and A. M. Vengsarkar, "Optical fiber long-period grating sensors," *Opt. Lett.* 21, 692, 1996.

[24] H. J. Patrick, A. D. Kersey, and F. Bucholtz, "Analysis of the Response of Long Period Fiber Gratings to External Index of Refraction," *J. Lightwave Technol.* 16, 1606, 1998.

[25] D. Flannery, S. W. James, R. P. Tatam, and G. J. Ashwell, "Fiber-Optic Chemical Sensing with Langmuir-Blodgett Overlay Waveguides," *Appl. Opt.* 38, 7370-7374, 1999.

[26] I. Del Villar, I. Matías, F. Arregui, and P. Lalanne, "Optimization of sensitivity in Long Period Fiber Gratings with overlay deposition," *Opt. Express* 13, 56-69, 2005.

[27] Z. Wang, J. Heflin, R. Stolen, and S. Ramachandran, "Analysis of optical response of long period fiber gratings to nm-thick thin-film coating," *Opt. Express* 13, 2808-2813, 2005.

[28] A. Cusano, A. Iadicicco, P. Pilla, L. Contessa, S. Campopiano, A. Cutolo, and M. Giordano, "Cladding mode reorganization in high-refractive-index-coated long-period gratings: effects on the refractive-index sensitivity," *Opt. Lett.* 30, 2536-2538, 2005.

[29] S. W. James and R. P. Tatam, "Optical fibre long-period grating sensors: Characteristics and applications," *Meas. Sci. Technol.*, vol. 14, pp. R49–R61, May 2003.

[30] Y. -P. Wang, D. N. Wang, and W. Jin, "CO_2 laser-grooved long period fiber grating temperature sensor system based on intensity modulation," *Appl. Opt.* 45, 7966-7970, 2006.

[31] Y. -J. Rao, Z. -l. Ran, X. Liao, and H. -y. Deng, "Hybrid LPFG/MEFPI sensor for simultaneous measurement of high-temperature and strain," *Opt. Express* 15, 14936-14941, 2007.

[32] X. Shu, L. Zhang, and I. Bennion, "Sensitivity Characteristics of Long-Period Fiber Gratings," *J. Lightwave Technol.* 20, 255, 2002.

[33] Y. J. Rao, S. F. Yuan, X. K. Zeng, D. K. Lian, Y. Zhu, Y. P. Wang, S. L. Huang, T. Y. Liu, G. F. Fernando, L. Zhang, and I. Bennion, "Simultaneous strain and temperature measurement of advanced 3-D braided composite materials using an improved EFPI/FBG system," *Opt. & Laser. In Eng.* 38, 557-566, 2002.

[34] Anemogiannis E, Glytsis EN and Gaylord TK, "Transmission characteristics of long-period fiber gratings having arbitrary azimuthal/radial refractive index variations," *J. Lightwave Techno.* 21, pp. 218-227, 2003.

[35] T. Erdogan, "Cladding-mode resonances in short- and long- period fiber gratings," *J. Opt. Soc. Amer. A*, vol. 14, pp. 1760-1773, May 1997.

[36] W.P. Jakubik, M.W. Urbanczyk, S. Kochowski, J. Bodzenta, "Bilayer structure for hydrogen detection in a surface acoustic wave sensor system," *Sens and Actuators B* 85 (2002) 265

[37] Z. Zhao, M.A. Carpenter, H. Xia and D. Welch, "All-optical hydrogen sensor based on a high alloy content palladium thin film," *sensors and actuators B* 113 (2006) 532-538.

[38] M. Slaman, B. Dam, M. Pasturel, D.M. Borsa, H. Schreuders, J.H. Rector and R. Griessen, "Fiber optic hydrogen detectors containing Mg-based metal hydrides," *sensors and actuators B* 123 (2007) 538.

[39] M. Pasturel, M. Slaman, H. Schreuders, J. H. Rector, D. M. Borsa, B. Dam, and R. Griessen, "Hydrogen absorption kinetics and optical properties of Pd-doped Mg thin films," *J. Applied physics.* 100, 023515, 2006.

[40] J.M. Corres, , I.R. Matias, I. del Villar and F.J. Arregui, "Design of pH Sensors in Long-Period Fiber Gratings Using Polymeric Nanocoatings," *IEEE Sensors.*, 7, pp. 455-463, 2007.

VITA

Tao Wei was born on September 23, 1983 in Nanjing, China. In June 2002, he obtained a bachelor's degree in Department of Mechanical Engineering from Nanjing University of Technology, Nanjing, China.

In August 2006, he enrolled at the University of Missouri-Rolla to pursue a master's degree in Department of Electrical and Computer Engineering under the guidance of Dr. Hai Xiao. He received his Master of Science Degree in Electrical Engineering in 2008.